

Understanding the approach to thermalization from the eigenspectrum of non-Abelian gauge theories

Harshit Pandey,¹ Ravi Shanker,¹ and Sayantan Sharma¹

¹*The Institute of Mathematical Sciences, a CI of Homi Bhabha National Institute, Chennai 600113, India*

We study some interesting aspects of the spectral properties of SU(3) gauge theory, both with and without dynamical quarks (QCD) at thermal equilibrium using lattice gauge theory techniques. By calculating the eigenstates of a massless overlap Dirac operator on the gauge configurations, we implement a gauge-invariant method to study spectral properties of non-Abelian gauge theories. We have unambiguously categorized Dirac eigenvalues into different regimes based on a quantity defined in terms of the ratios of nearest neighbor spacings. While majority of these eigenstates below the magnetic scale are similar to those of random matrices belonging to the Gaussian Unitary ensemble at temperatures much higher than the chiral crossover transition in QCD, a few among them start to become prominent only near the crossover. These form fractal-like clusters with the median value for their fractal dimensions hinting at the universality class of the chiral transition in QCD. We further demonstrate that momentum modes below the magnetic scale in a particular non-equilibrium state of QCD are classically chaotic and estimate an upper bound on the thermalization time ~ 1.44 fm/c by matching this magnetic scale with that of a thermal state at ~ 600 MeV.

PACS numbers: 12.38.Gc, 11.15.Ha, 11.30.Rd, 11.15.Kc

Introduction The eigenspectrum of the Hamiltonian of an isolated quantum system provides valuable insights not only on dynamical properties such as their approach to thermalization but also their properties in thermal equilibrium through the eigenstate thermalization hypothesis (ETH) [1–4]. Bohigas, Giannoni and Schmit (BGS) conjectured that [5] quantum fluctuations of the eigen level-spacing distributions whose classical dynamics is chaotic can be described, based on symmetries, by one of three distinct Wigner classifications of random matrix theory (RMT). Whereas this conjecture has been verified in spin systems with different global as well as local symmetries but no such verification exists yet for non-Abelian gauge theories. Generic quantum systems, however, have a much richer spectrum owing to the melding of regular levels with the chaotic ones [6] due to which the realization of BGS conjecture is non-trivial [7]. Furthermore, eigenstates with universal RMT fluctuations may provide a route towards thermalization in (strongly) interacting isolated quantum systems [8, 9].

Notwithstanding the challenge to construct a quantum Hamiltonian for non-Abelian gauge theories like QCD, studying its spectral properties is important to understand how such systems with strong color (gauge) interactions thermalize. This is relevant for addressing questions like, in what time scale will the fireball formed in a relativistic heavy-ion collision or the quarks and gluons in the early universe thermalize [10, 11]. In the latter case, this is crucial for understanding nucleosynthesis of light elements that accounts for $\sim 99\%$ of the visible matter in the present universe. It will also be important to investigate, once thermalized, if spectral properties of QCD have some imprints of the universal features related to chiral symmetry restoration at QCD phase transition, even though the universal critical part of thermodynamic

quantities like free energy may be subdominant compared to its regular part for physical quark mass.

From ab-initio lattice field theory simulations it is now established that thermal non-Abelian SU(3) gauge theory coupled to two dynamical light quarks and a heavier strange quark that transform under the fundamental representation of the gauge group undergoes a smooth crossover transition [12–16]. This is due to the fact that QCD with two light quarks has an almost exact non-singlet $SU_V(2) \times SU_A(2)$ chiral symmetry which breaks into its $SU_V(2)$ subgroup below a pseudo-critical temperature $T_c = 156.5(1.5)$ MeV [17]. The confinement of color degrees of freedom also happens around the same temperature [18], leading to the formation of color-singlet baryon and meson states. The singlet $U_A(1)$ part of chiral symmetry, though anomalous, is believed to affect the nature of the phase transition in QCD with two light quark [19] flavors depending on its *effective* magnitude at T_c , and is an ongoing area of research [20–33]. Specific features of the Euclidean Dirac eigenvalue spectrum in QCD can successfully explain the breaking or restoration of the non-singlet chiral symmetry [34, 35]. In absence of any conclusive evidence on whether the $U_A(1)$ is restored *effectively* with its non-singlet counterpart at the same temperature, one might ask if any specific features of the eigenspectrum in QCD can provide a fresh perspective on this matter.

In this Letter, we motivate and show how some specific features of the QCD Dirac eigenspectrum can give us important insights to address these unresolved issues. In the Dirac spectrum, the localized and the chaotic regions can be separated out which allows us to provide a first demonstration of the realization of BGS conjecture in a non-Abelian gauge theory in three spatial dimensions using lattice techniques. For this, we show using some discern-

ing observables that the eigenstates of the Dirac operator in 2+1 flavor QCD with eigenvalues below the magnetic scale [36] at a temperature $T \simeq 624$ MeV, have spectral properties consistent with a particular RMT universality. There also exists a particular non-equilibrium state where the low-momentum single-particle gluon states below the corresponding magnetic scale are densely occupied, hence classical [37–39] and is chaotic, characterized by a positive Lyapunov exponent. A crucial observation from our study is that both in the classical non-thermal state as well as in the quantum (thermal) state of QCD at high temperatures, these single-particle states of gluons below the non-perturbative *magnetic* scale [36] have the same physical properties akin to a chaotic system. Matching the scales that define these states enables us to provide an upper bound for the thermalization time $\simeq 1.44$ fm/c to arrive at the thermal state described by $T \simeq 624$ MeV, starting from the over-occupied non-thermal state.

The presence of light dynamical fermions (quarks) does not affect our procedure of matching scales since the chaoticity inherent in the spectrum, evident from the universal fluctuations akin to RMT, is a property of the non-Abelian color group. Rather, their presence only contributes to the magnitude of the *magnetic* scale through the running of the coupling, thus ensuring a faster thermalization of the magnetic gluons. Once thermalized, the role of dynamical quarks becomes more important close to the chiral crossover transition. We study how the spectral properties of the thermal states change as the temperature is cooled down to T_c where the presence of dynamical light quarks indeed becomes increasingly relevant in determining the structural properties of the infrared eigenstates and thus driving the chiral crossover transition. The properties of the eigenspectrum of QCD Dirac operator on thermal states of QCD as a function of temperature are discussed in the third section after briefly describing our numerical setup. The subsequent sections discuss the properties of a particular non-thermal state of QCD thus building upon the discussion on estimating an upper bound on the thermalization time for the magnetic gluons in QCD. We conclude by discussing the implications of our study.

Numerical Set-up The thermal partition function of QCD, written in terms of its quantum Hamiltonian H_{QCD} as $\text{Tr} [e^{-H_{\text{QCD}}/T}]$, can be equivalently represented as a path integral in the configuration space of fermions and gauge fields, weights of which are determined by $e^{-S_{\text{QCD}}}$, where S_{QCD} is the classical action in Euclidean spacetime with a compact *fictitious* time direction τ of extent $1/T$. If a probe massless quark is in thermal equilibrium with these gauge fields, the information encoded in the eigenspectrum of the QCD Hamiltonian, e.g., the universal level spacing fluctuations, will be contained in its Dirac eigenspectrum as well [40].

In order to study the Dirac eigenspectrum of QCD with two light and one heavier strange quark, we have used

gauge configurations generated using the Möbius domain wall discretization for fermions [41] which respects chiral symmetry on the lattice to a very good extent. This particular domain wall fermion discretization allowed us to work with a moderately small fifth-dimensional extent, $L_5 = 16$ and the Möbius parameters b_5 and c_5 were chosen such that $b_5 - c_5 = 1$. The values of c_5 at different temperatures are listed in Table I, which were chosen such that the chiral symmetry violation for our chosen L_5 is minimal. The domain wall height M_5 , was kept fixed at 1.8 for the entire set of simulations. The bare light and strange quark masses were chosen such that the pion mass is physical i.e. $M_\pi \sim 135$ MeV and so is the kaon mass with $M_K \sim 495$ MeV [15]. For $T \lesssim 186$ MeV we have partly used the existing gauge configurations generated by the HotQCD collaboration [15] and a few from Ref. [42] whereas the configurations for $T = 195$ MeV were generated by us choosing the same set of parameters used in Ref. [15].

We have worked with a fixed lattice size with $N_s = 32$ sites along each spatial direction and $N_\tau = 8$ sites along the Euclidean temporal direction. The range of temperatures, $T = 1/(N_\tau a)$, we have studied is between 149-195 MeV, where a is the lattice spacing, such that the spatial extent $L = V^{1/3}$ is ~ 5.3 fm for $T = 149$ MeV whereas $L \sim 4$ fm for the highest temperature $T = 195$ MeV. We use the massless overlap Dirac operator [43, 44] defined as $D_{ov} = 1 + \gamma_5 \text{sign}(\gamma_5 D_w(-M_5))$ where $D_w(-M_5)$ is the Wilson Dirac operator with the domain wall height $M_5 = 1.8$ (appearing as a negative mass parameter) as a probe to measure the eigenspectrum of the QCD configurations. This is because the overlap Dirac operator has an exact chiral symmetry on the lattice. For the implementation of the matrix-sign function, we have calculated the lowest 30 eigenvectors of $D_w^\dagger D_w$. The sign function was computed exactly in the vector space spanned by first 30 eigenvectors of the Wilson Dirac operator and approximated in terms of a Zolotarev rational polynomial with 25 terms in the rest of the vector space. The numerical precision of the matrix sign-function was such that its norm-squared deviated from unity at $\sim 10^{-9}$ - 10^{-10} and the resultant overlap Dirac operator satisfied the Ginsparg-Wilson relation at a precision $\sim 10^{-10}$. We have calculated the first ~ 100 eigenvalues of the overlap Dirac operator using the Kalkreuter-Simma Ritz algorithm [45]. We have also generated thermalized SU(3) gauge configurations (without dynamical quarks) with Wilson gauge action on $32^3 \times 8$ lattice and inverse coupling $\beta = 6/g^2 = 6.545$, which corresponds to a temperature $T \simeq 624$ MeV, about twice the deconfinement temperature $T_d \simeq 312$ MeV [46, 47]. The scale $r_0 = 0.4701(36)$ fm [48] is used to set the temperature in this case. At this temperature the gluon degrees of freedom, especially below the magnetic scale are dominant, thus these gauge ensembles represent the physical scenario. The details about the number of eigenvalues

computed and the number of configurations used at each temperature in this study are summarized in Table I.

The SU(3) gauge configurations at high temperatures were generated in order to compare how different a thermalized state is from a classical state of QCD which consists of highly occupied gauge fields [39, 49] with a non-thermal phase space distribution and without dynamical quarks. For generating these non-thermal, classical gauge configurations on a three-dimensional lattice using Hamiltonian evolution, we choose the lattice extent with $N = 64$ sites along each spatial direction, with lattice spacing in units of the gluon saturation scale $Q \sim 1.5$ GeV to be $Qa_s = 0.25$ such that the spatial extent in physical units is ~ 2.1 fm. This is to ensure that we have a sufficiently large volume and enough number of momentum modes of gauge fields in the deep-infrared part of its momentum distribution.

2+1 flavor QCD						
T (MeV)	β	c_5	N_s	N_τ	N_{eigen}	$N_{\text{conf}s}$
149	1.671	1.5	32	8	100	40
159	1.707	1.5	32	8	100	44
164	1.725	1.5	32	8	100	95
177	1.771	1.0	32	8	100	93
186	1.801	1.0	32	8	90	57
195	1.829	0.9	32	8	100	101
SU(3)						
624	6.545	—	32	8	100	46

Tab. I. Number of gauge configurations studied at different temperatures (corresponding to the values of $\beta = 6/g^2$) and the lattice sizes used in this work. The table also lists the number of overlap Dirac eigenvalues calculated per gauge configuration, along with the values of the Möbius parameter c_5 used in the generation of gauge ensembles at each temperature.

Properties of eigenvalue spectrum of gauge theories in thermal equilibrium We study the spectral properties of the four-dimensional overlap Dirac operator of a probe massless quark whose eigenvalues are denoted as λ_n where n is an integer whose maximum value is the dimension of the Dirac operator. This is a gauge-invariant procedure to understand the spectral properties of QCD non-perturbatively. The fluctuations of level spacings between consecutive eigenvalues are universal and belong to one of the three Wigner surmises if the system is chaotic. An important observable of interest to study these fluctuations is $\langle \tilde{r} \rangle$, where \tilde{r}_n is defined [50] as $\tilde{r}_n = \min\left(r_n, \frac{1}{r_n}\right)$. The quantity $r_n = \frac{s_{n+1}}{s_n}$ represents the ratio between two consecutive level spacings $s_n = \lambda_{n+1} - \lambda_n$. The observable $\langle \tilde{r} \rangle$ is obtained by averaging over \tilde{r}_n for all eigenvalues within a spectral window and subsequently over the entire ensemble of gauge configurations at a particular temperature. For this reason,

the index n is explicitly dropped after performing these averages while calculating $\langle \tilde{r} \rangle$. There is a distinct advantage of choosing $\langle \tilde{r} \rangle$ over other observables discussed in the literature [51] to characterize the eigenvalue spectrum. This is due to the fact that, unlike observables which are integrated quantities of level-spacing distributions and thus require unfolding to remove the system-dependent mean, the quantity $\langle \tilde{r} \rangle$ does not suffer from such systematic uncertainties.

We now elucidate our procedure to categorize different spectral windows. We first calculate $\langle \tilde{r} \rangle$ in each small bins of λ/T by averaging over the gauge configurations at each temperature. We then checked if the values of $\langle \tilde{r} \rangle$ are exactly similar within errors to that obtained for random matrices belonging to a Gaussian Unitary Ensemble (GUE) for some of the bins. Such bins then define a particular spectral window. For $T < T_c$, and for $T \sim 2T_d$ the values of $\langle \tilde{r} \rangle$ measured in all the bins are consistent within errors with $\langle \tilde{r} \rangle = 0.60266$ obtained for the GUE. We observe a similar agreement for all bins within the spectral windows defined by $\lambda/T > 0.08, 0.12, 0.33, 0.5, 0.6$ at temperatures $T = 159, 164, 177, 186, 195$ MeV respectively. We note here that the upper cutoff to these spectral windows is decided by the maximum eigenvalue that we have calculated at a particular temperature. We henceforth refer to them as *bulk eigenmodes* and their resulting $\langle \tilde{r} \rangle$ as a function of T/T_c are shown as red points in the left panel of Fig. 1. These bulk eigenmodes thus characterize the chaotic part of the QCD Dirac eigen-spectrum.

We next define *intermediate eigenmodes* which belong to the spectral window characterized by λ/T between 0.0-0.08 for $T = 159$ MeV, 0.0-0.12 for $T = 164$ MeV, 0.0-0.33 for $T = 177$ MeV, 0.0-0.5 for $T = 186$ MeV and 0.0-0.6 for $T = 195$ MeV, for which the $\langle \tilde{r} \rangle$ for all the bins within the spectral window lies between the GUE prediction and the corresponding value for completely uncorrelated eigenvalues. The emergence of these intermediate eigenmodes near T_c , shown as blue points in the left panel of Fig. 1, has important physical consequences which we will discuss in the later part of this section.

To verify that the bulk eigenmodes are correctly identified and the robustness of our procedure, we next measure the probability distribution of nearest neighbor spacing ratios [52] since this quantity is also independent of the unfolding procedure and can be directly matched with the GUE prediction given by $P(r) = \frac{11.16 (r+r^2)^2}{(1+r+r^2)^4}$. In the right panel of Fig. 1, we observe that the bulk eigenmodes defined using our criterion indeed follow the GUE prediction for all temperatures. The spectral window that defines the bulk eigenmodes is similar to our earlier studies of the continuum extrapolated level spacing distribution in QCD with the staggered Dirac discretization [30].

We next study the localization properties of the Dirac

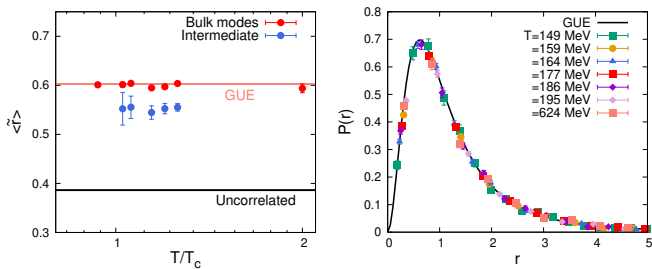


Fig. 1. Left panel: Average value $\langle \bar{r} \rangle$ in different spectral windows defined in terms of the overlap Dirac eigenvalues at various temperatures T . Red and blue points correspond to bulk and intermediate eigenmodes, respectively. The results are compared with the theoretical expectations for the GUE and completely uncorrelated (Poisson) spectra, shown as red and black horizontal lines, respectively. Right panel: Probability distribution of ratios of consecutive level spacings for bulk eigenmodes at different temperatures with and without dynamical quarks. Note that for pure SU(3) gauge ensemble at $T = 624$ MeV, the T_c represents the deconfinement temperature T_d .

eigenstates, which for a particular eigenstate $\psi(\mathbf{x})$ is quantified with the generalized Rényi entropy defined as,

$$R_\alpha = \frac{1}{1-\alpha} \ln \sum_{\mathbf{x}} p_{\mathbf{x}}^\alpha, \quad 1 \leq \alpha < \infty. \quad (1)$$

The quantity $p_{\mathbf{x}} = |\psi(\mathbf{x})|^2$ denotes the probability density of an eigenstate at a spatial position \mathbf{x} obtained after averaging the four-dimensional density over τ . From the top panel of Fig. 2 it is evident that the bulk eigenmodes have significantly higher values of the first Rényi entropy R_1 ranging between $0.92 < R_1/\log V < 1.0$, approaching unity at the highest temperature i.e. 624 MeV. This implies that the bulk eigenmodes are almost completely delocalized over the spatial volume and thus are ergodic, containing equivalent thermal information in each of them. This is an indirect manifestation [4] of the ETH, which has been demonstrated in non-Abelian theories in 2+1 dimensions [53, 54]. Whereas close to T_c at $T = 159, 164, 177, 186, 195$ MeV, the intermediate eigenmodes do not contain the entire thermodynamic information that is encoded in the bulk eigenmodes, as evident from their values of $R_1/\log V$. These intermediate eigenmodes are thus not as delocalized as bulk eigenmodes, hence not fully ergodic. We will next discuss the implications of this observation.

To further understand the structure of the intermediate eigenmodes, we study the inverse participation ratio (IPR) defined as $P_2 = \sum_{\mathbf{x}} |\psi(\mathbf{x})|^4$. For a completely delocalized eigenstate we expect P_2 to scale as the inverse of the volume of the system as L^{-3} but may not achieve this scaling even in the deep bulk due to the presence of thermal fluctuations. The plot of $D_2 = -\log P_2/\log L$ as a function of bins in λ/T shown in the lower panel of Fig. 2 demonstrates different volume scaling for the

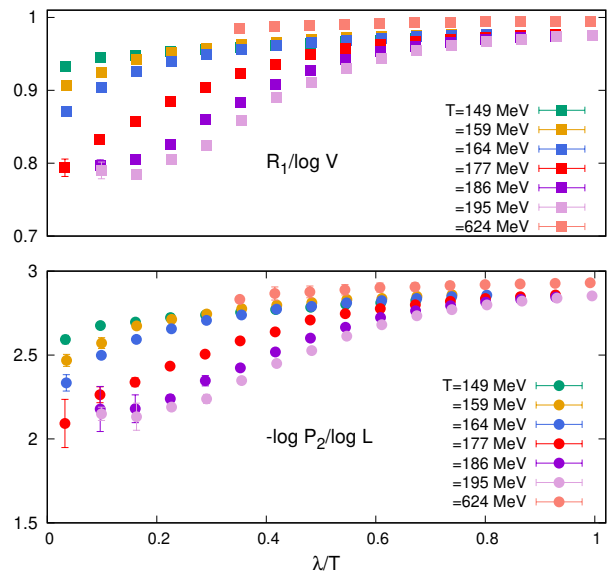


Fig. 2. Variation of first Rényi entropy (top panel) and D_2 (bottom panel), for eigenvectors binned in λ/T for different temperatures, performed on the gauge configurations mentioned in table I.

bulk and intermediate eigenmodes. To further quantify this scaling we calculate the distribution of the fractal dimension, D_f of the eigenvectors, in the eigenvalue intervals used earlier to characterize the intermediate and bulk eigenmodes instead of D_2 , because of the low statistics. However both of these quantities contain equivalent information about the scaling of the eigenmodes. We have calculated the fractal dimension of an eigenstate using the box-counting method [55] where the threshold for the probability density is chosen to be $0.75/V$, since this choice yields a scaling behavior that is consistent with D_2 within errors across all λ/T bins. The probability distribution in Fig. 3 of the fractal dimension D_f has been constructed using an error-weighted Gaussian smearing method, where the data is extracted from a Gaussian distribution centered at each measured value of D_f with a width given by its error. These data are summed and normalized such that the area under the curve is unity, thus producing a smooth probability distribution function instead of discrete histograms. As evident from Fig. 3, the fractal dimensions of the bulk eigenmodes for all temperatures are significantly higher than the intermediate eigenmodes, the median values ranging between $2.78 \lesssim D_f \lesssim 2.84$. For the temperature range $\gtrsim T_c$, the D_f of the intermediate eigenvectors show a sensitivity to temperature variation thus reflecting the physical changes occurring in the system due to the chiral crossover transition. The probability distribution of D_f denoted by $P(D_f)$ has a spread due to the fact that fluctuations can exist on all length scales larger than the lattice spacing resulting in wavefunctions with different extent of delocalization to co-exist [56],

with median values of $D_f = 2.52, 2.49, 2.52, 2.55$ at $T = 164, 177, 186, 195$ MeV respectively, for the intermediate region. The median value of D_f just above the thermal crossover transition can be interpreted using the relation $D_f = 3 - \beta/\nu$ [57]. If we put in the critical exponents β, ν of a three-dimensional $O(4)$ spin model [58], the value of $D_f \simeq 2.485$, which is similar to the median values of D_f of the intermediate eigenvectors.

The presence of small kinks in the probability distribution of D_f at $T \gtrsim 186$ MeV is expected due to the rare occurrence of near-zero modes at high temperatures, hence one would require larger statistics to obtain a smooth curve. One also observes a spread of $P(D_f)$ towards lower values of $D_f \simeq 2$ with increasing temperatures, indicating the appearance of localized eigenmodes. With this trend we expect that at even higher temperatures, localized eigenmodes characterized by $\langle \tilde{r} \rangle$ close to the value in a uncorrelated Poissonian distribution would contribute significantly to the broadening of $P(D_f)$. This can be related to the observation of the Anderson-Mott transition and the existence of a mobility edge at high temperatures [40, 51, 59–67]. Eventually the low-lying eigenstates near or below the mobility edge, will exhibit a median value of fractal dimension similar to that in a 3-dimensional Anderson model [40].

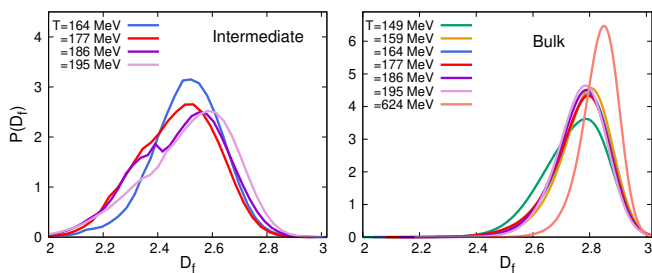


Fig. 3. Probability distribution of the fractal dimension D_f at different temperatures and in eigenvalue intervals characterized as the intermediate (left panel) and the bulk eigenmodes (right panel).

To summarize, all eigenvalues of the Dirac operator we have measured are below the magnetic scale $g^2 T/\pi$ [36] and are inherently non-perturbative in nature. Away from the crossover transition, these (bulk) eigenmodes are delocalized almost over the entire volume albeit with local thermal fluctuations, consistent with RMT. However approaching the crossover transition results in the appearance of the fractal-like intermediate eigenmodes, which carry information about the chiral phase transition, which could be of $O(4)$ universality [29, 30, 68]. These eigenmodes are prominently detectable in a temperature range where there are proposals of an IR conformal phase [32, 69–74], appearance of emergent symmetries [75, 76] and their eventual disappearance can explain the *effective* restoration of $U_A(1)$ subgroup of chiral symmetry [30]. The occurrence of percolating clusters of

Polyakov loop [77, 78], has been reported earlier in another context, near the deconfinement phase transition in gauge theories without dynamical quarks. Furthermore, the connection between phase transitions and fractals has also been discussed in the context of spin systems, e.g., in the Ising model [79].

Properties of a non-equilibrium state of $SU(3)$

Since the thermal state in QCD at high temperatures exhibits spectral properties corresponding to a random matrix theory, we next investigate if there is a classical state that exhibits chaos. Inspired by the Color Glass Condensate effective theory description of QCD [38], where the typical gluon momenta are close to the saturation scale Q , which satisfies the condition $Q^2 \gg \Lambda_{QCD}^2$, we start with an initial classical state of the non-Abelian $SU(3)$ gauge theory characterized by the phase-space distribution $g^2 f_g(|\mathbf{p}|, t=0) = n_0 \frac{Q}{|\mathbf{p}|} e^{-\frac{|\mathbf{p}|^2}{2Q^2}}$. This initial state is clearly athermal and represents a typical over-occupied infrared sector of QCD, characterized by classical gluons whose occupation numbers $\sim n_0/g^2$ are non-perturbatively large (since g is very small) [49]. Starting with this initial condition, the gauge links $U_{i,\mathbf{x}}$ and its conjugate momenta i.e. electric fields $E_{a,\mathbf{x}}^i$ are evolved in time according to classical Hamiltonian equations of motion denoted by

$$\frac{\partial U_{i,\mathbf{x}}}{\partial t} = \frac{\partial H}{\partial E_{i,\mathbf{x}}}, \quad \frac{\partial E_{i,\mathbf{x}}}{\partial t} = -\frac{\partial H}{\partial U_{i,\mathbf{x}}}, \quad i = 1, 2, 3. \quad (2)$$

Hamilton's equations are written in the temporal-axial gauge $A_0(\mathbf{x}) = 0$. It is well known that such a system undergoes a rapid memory loss [39, 80] of their initial conditions and subsequently enter a self-similar scaling regime where the gluon distribution function exhibits a scaling relation of the form, $g^2 f_g(|\mathbf{p}|, t) = (Qt)^{-\frac{4}{7}} f_s \left[(Qt)^{-\frac{1}{7}} \frac{|\mathbf{p}|}{Q} \right]$, characteristic of a non-thermal fixed point of the classical evolution. Within such a scaling regime, one observes a separation of scales [81] where the hard (ultraviolet) scale is distinctly separated from the electric and the (deep-infrared) magnetic scales similar to what is observed in equilibrium gauge theories at high temperatures. How such a system achieves thermal equilibrium is not well understood, though kinetic theories that share similar scaling properties determined by the same critical exponents can be identified [49, 82].

We next study the properties of the non-Abelian gauge theory within this self-similar scaling regime in particular, whether it exhibits chaotic behavior. We study the separation of gauge trajectories in the phase space characterized by a gauge-invariant distance measure [83] defined as $D(U_l, U'_l, t) = \frac{1}{N_P} \sum_P \frac{1}{N_c} |\text{tr} U_P - \text{tr} U'_P|$, in terms of the difference between the expectation values of the plaquettes U_P and U'_P measured a time t starting from infinitesimally close initial conditions at $t=0$ given by n_0 and $n_0 + \Delta n_0$, $\Delta n_0 = 0.001$. The trace is performed over the color degrees of freedom. The results obtained

for the distance function are shown in the inset of Fig. 4. It is evident that the system shows a chaotic behavior where $D(t)$ increases exponentially with time, saturating at later times due to finite gauge-space volume. Fitting this initial growth as a function of time with the ansatz, $D(t) = D_0 \exp(\gamma t)$ we obtain a positive (largest) Lyapunov exponent γ characteristic of a chaotic system for a wide range of initial gluon energy densities ε/Q^4 shown in Fig. 4, given by $\varepsilon \propto n_0/g^2$. For the range of energy densities, γ/Q grows linearly as the fourth root of energy density with the best fit given by

$$\gamma/Q = 0.0400(7) \times (\varepsilon/Q^4)^{0.24(3)}. \quad (3)$$

Since the Lyapunov exponent characterizes how fast the gluon trajectories will spread out over the entire phase space, its inverse can give a rough estimate of the typical thermalization time [84, 85].

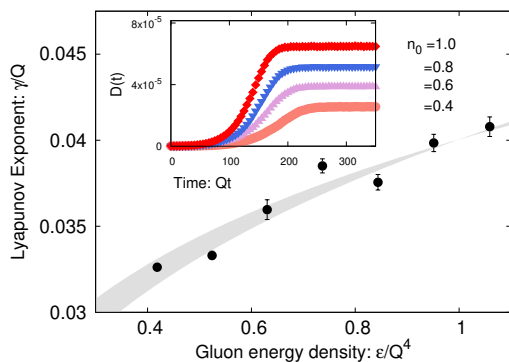


Fig. 4. Scaling of the Lyapunov exponent γ for SU(3) with the energy density ε . The exponential growth of the distance function $D(t)$ between two classical trajectories in the gauge space for different values of initial gluon density is shown in the inset.

Implications of our study for thermalization of non-Abelian gauge theories Establishing that a particular classical state of SU(3) gauge theory which exhibits a non-thermal scaling property in its phase-space distribution, is chaotic we now discuss its implications for thermalization. Within this self-similar scaling regime, the magnetic ($\sqrt{\sigma}$), electric (m_D) and the hard (Λ) scales evolve with time according to the following relations: $\sqrt{\sigma}(t) \sim Q(Qt)^{-3/10}$, $m_D(t) \sim Q(Qt)^{-1/7}$ and $\Lambda(t) \sim Q(Qt)^{1/7}$ [86]. On the other hand, for SU(3) gauge theory at thermal equilibrium at $T \simeq 624$ MeV, the magnetic, electric, and hard scales are $g^2T/\pi = 0.81T$, $gT = 1.61T$ and πT respectively. The strong coupling g in this work is measured at the scale πT using the five-loop β -function [87]. In order to estimate the thermalization time starting from a self-similar scaling regime and ending at a thermal fixed point, we measure how long it takes for the magnetic scale $\sqrt{\sigma}(t)$ to evolve to its value in a thermal plasma. This is motivated by the fact that the

gauge momentum modes whose momenta are less than the magnetic scale are over-occupied and exhibit chaotic behavior both in the classical as well as in the quantum (thermal) regime. If one assumes that thermalization is achieved at a typical temperature $T \simeq 624$ MeV, the evolution of the magnetic scale to its thermal value denoted by $Q(Q\tau_{th})^{-3/10} = 0.81T$ gives an estimate of the thermalization time $\tau_{th} \approx 5.2$ fm/c. Incidentally, this estimate is close to that obtained from the inverse of Lyapunov exponent $\gamma^{-1} \sim 4.9(1)$ fm/c measured at a typical energy density $\varepsilon = 0.209 Q^4$ which is closest in magnitude to the thermal plasma at $T \simeq 624$ MeV and also close to the estimates obtained from entropy production arguments [83, 88].

Interestingly, though, the presence of dynamical fermions does not affect the universality in spectral properties of QCD below the magnetic scale (see Fig. 1) or quantities like the spatial string tension $\sqrt{\sigma}$, even in the non-thermal state. This comes from the fact that $\sqrt{\sigma}$ only increases by $\sim 1.6\%$ in the presence of dynamical quarks [89] in QCD at thermal equilibrium for $T > 600$ MeV. Fermion production is an inherent quantum process that will pull the system out from the athermal classical fixed point to the thermal one and would facilitate fast thermalization. This can be understood from the fact that the presence of dynamical quarks increases the magnitude of the magnetic scale in a thermal system by modifying the running of the gauge coupling with energy. At temperature $T \simeq 624$ MeV, the presence of dynamical quarks leads to an enhancement in the magnetic scale to $g^2T/\pi = 1.19T$ which is ~ 1.5 times compared to its value in gauge theory without fermions. The effect on the thermalization time is dramatic since it varies with the ratio of magnetic scales as $(0.81/1.19)^{10/3}$. The fermions thus facilitate a faster rate of thermalization, resulting in a $\tau_{th} = 1.44$ fm/c which is about $\sim 28\%$ of that estimated earlier in gauge theory without fermions. This upper bound estimate of τ_{th} reported here is smaller compared to the typical thermalization time-scales ~ 3 fm/c estimated using perturbative QCD scattering processes [90].

Conclusions & Outlook Over the years, the features inherent in the Dirac eigenspectrum have provided us with key insights on the chiral, topological and localization properties of QCD [40, 91, 92]. In this Letter, we discuss two interesting aspects of the Dirac spectrum of QCD and their physical implications. Firstly, in QCD with 2 + 1 flavors of physical quarks, extended eigenvectors percolating over the entire volume start to become prominent just above T_c which show intermediate level statistics between opposite extremes of an RMT and uncorrelated eigenvalues. Though the transition associated with chiral symmetry breaking is a smooth crossover and hence there is no unique order parameter, however the structural features of the eigenvectors close to T_c are observed to carry information about the universality class. This is evident from the fact that the median values of the

fractal dimensions of these intermediate eigenmodes are consistent with $O(4)$ universality. Secondly, we demonstrate a non-trivial realization of the BGS conjecture in non-Abelian $SU(3)$ gauge theory, by measuring its single-particle states with the Dirac operator defined on these gauge links. Whereas eigenstates of the Dirac operator measured on a thermal (quantum) QCD configuration which are deep in the bulk, but with eigenvalues below the magnetic scale $g^2 T/\pi$, exhibit level-spacing ratios consistent with random matrices of the Gaussian unitary ensemble, there exists a classical non-thermal state of magnetic gluons which is chaotic. Establishing this fact allows us to naturally ask the follow-up question: How long does it take for the chaotic system consisting of magnetic gluons to thermalize?

Defining thermalization time as how fast these soft single-particle momentum states acquire a thermal distribution starting from an over-occupied state of gluons where single-particle momentum distribution exhibits a self-similar scaling, we obtain an upper bound of ~ 1.44 fm/c to reach to a thermal state at $T \simeq 624$ MeV by matching the (magnetic) scales, below which these states are defined. The inclusion of dynamical fermions only results in an efficient separation of scales at these high temperatures, thus allowing for such a fast thermalization of the non-perturbative but classical infrared (magnetic) modes of QCD. It would nonetheless be interesting to verify this picture with quantum simulations of dynamical quarks with gauge interactions which could be feasible in lower dimensions in the coming years.

Acknowledgements We are grateful to Soumya Bera, Sumilan Banerjee, Frithjof Karsch, V. K. B. Kota, Hridis K. Pal and Soeren Schlichting for helpful suggestions and discussions during the course of this work. We are indebted to Frithjof Karsch and Soeren Schlichting for their kind hospitality at the Theoretical Physics Group, Bielefeld University when this work was being finalized. This work is in part supported by the Deutsche Forschungsgemeinschaft (DFG, German Research Foundation) - Project number 315477589-TRR211. We thank the HotQCD collaboration, formerly also consisting of members from the RBC-LLNL collaboration, for sharing some of the gauge configurations with us. The authors acknowledge the computing time provided by the Computing Center at the Institute of Mathematical Sciences. Our GPU code is in part based on some of the publicly available QUDA libraries [93].

[1] J. M. Deutsch, Phys. Rev. A **43**, 2046 (1991).

[2] M. Srednicki, Phys. Rev. E **50** (1994), 10.1103/PhysRevE.50.888, arXiv:cond-mat/9403051.

[3] H. Tasaki, Phys. Rev. Lett. **80**, 1373 (1998).

[4] M. Rigol, V. Dunjko, and M. Olshanii, Nature **452**, 854 (2008), arXiv:0708.1324 [cond-mat.stat-mech].

[5] O. Bohigas, M. J. Giannoni, and C. Schmit, Phys. Rev. Lett. **52**, 1 (1984).

[6] M. V. Berry and M. Robnik, Journal of Physics A: Mathematical and General **17**, 2413 (1984).

[7] O. Bohigas, S. Tomsovic, and D. Ullmo, Phys. Rev. Lett. **65**, 5 (1990).

[8] A. Polkovnikov, K. Sengupta, A. Silva, and M. Vengalattore, Reviews of Modern Physics **83**, 863 (2011).

[9] R. Nandkishore and D. A. Huse, Annual Review of Condensed Matter Physics **6**, 15 (2015).

[10] S. Schlichting and D. Teaney, Ann. Rev. Nucl. Part. Sci. **69**, 447 (2019), arXiv:1908.02113 [nucl-th].

[11] J. Berges, M. P. Heller, A. Mazeliauskas, and R. Venugopalan, Rev. Mod. Phys. **93**, 035003 (2021), arXiv:2005.12299 [hep-th].

[12] Y. Aoki, G. Endrodi, Z. Fodor, S. D. Katz, and K. K. Szabo, Nature **443**, 675 (2006), arXiv:hep-lat/0611014.

[13] A. Bazavov *et al.*, Phys. Rev. D **85**, 054503 (2012), arXiv:1111.1710 [hep-lat].

[14] A. Bazavov *et al.* (HotQCD), Phys. Rev. D **90**, 094503 (2014), arXiv:1407.6387 [hep-lat].

[15] T. Bhattacharya *et al.*, Phys. Rev. Lett. **113**, 082001 (2014), arXiv:1402.5175 [hep-lat].

[16] F. Burger, E.-M. Ilgenfritz, M. P. Lombardo, and A. Trunin, Phys. Rev. D **98**, 094501 (2018), arXiv:1805.06001 [hep-lat].

[17] A. Bazavov *et al.* (HotQCD), Phys. Lett. B **795**, 15 (2019), arXiv:1812.08235 [hep-lat].

[18] A. Bazavov, N. Brambilla, H. T. Ding, P. Petreczky, H. P. Schadler, A. Vairo, and J. H. Weber, Phys. Rev. D **93**, 114502 (2016), arXiv:1603.06637 [hep-lat].

[19] R. D. Pisarski and F. Wilczek, Phys. Rev. D **29**, 338 (1984).

[20] S. Aoki, H. Fukaya, and Y. Taniguchi, Phys. Rev. D **86**, 114512 (2012), arXiv:1209.2061 [hep-lat].

[21] A. Bazavov *et al.* (HotQCD), Phys. Rev. D **86**, 094503 (2012), arXiv:1205.3535 [hep-lat].

[22] A. Tomiya, G. Cossu, S. Aoki, H. Fukaya, S. Hashimoto, T. Kaneko, and J. Noaki, Phys. Rev. D **96**, 034509 (2017), [Addendum: Phys.Rev.D 96, 079902 (2017)], arXiv:1612.01908 [hep-lat].

[23] V. Dick, F. Karsch, E. Laermann, S. Mukherjee, and S. Sharma, Phys. Rev. D **91**, 094504 (2015), arXiv:1502.06190 [hep-lat].

[24] B. B. Brandt, A. Francis, H. B. Meyer, O. Philipsen, D. Robaina, and H. Wittig, JHEP **12**, 158 (2016), arXiv:1608.06882 [hep-lat].

[25] P. Petreczky, H.-P. Schadler, and S. Sharma, Phys. Lett. B **762**, 498 (2016), arXiv:1606.03145 [hep-lat].

[26] S. Aoki, Y. Aoki, G. Cossu, H. Fukaya, S. Hashimoto, T. Kaneko, C. Rohrhofer, and K. Suzuki (JLQCD), Phys. Rev. D **103**, 074506 (2021), arXiv:2011.01499 [hep-lat].

[27] H. T. Ding, S. T. Li, S. Mukherjee, A. Tomiya, X. D. Wang, and Y. Zhang, Phys. Rev. Lett. **126**, 082001 (2021), arXiv:2010.14836 [hep-lat].

[28] S. Aoki, Y. Aoki, H. Fukaya, S. Hashimoto, C. Rohrhofer, and K. Suzuki (JLQCD), PTEP **2022**, 023B05 (2022), arXiv:2103.05954 [hep-lat].

[29] O. Kaczmarek, L. Mazur, and S. Sharma, Phys. Rev. D **104**, 094518 (2021), arXiv:2102.06136 [hep-lat].

[30] O. Kaczmarek, R. Shanker, and S. Sharma, Phys. Rev. D **108**, 094501 (2023), arXiv:2301.11610 [hep-lat].

[31] T. G. Kovacs, Phys. Rev. Lett. **132**, 131902 (2024),

- arXiv:2311.04208 [hep-lat].
- [32] A. Alexandru, C. Bonanno, M. D'Elia, and I. Horváth, (2024), arXiv:2404.12298 [hep-lat].
- [33] M. Giordano, (2024), arXiv:2404.03546 [hep-lat].
- [34] A. V. Smilga and J. Stern, Phys. Lett. B **318**, 531 (1993).
- [35] J. J. M. Verbaarschot and I. Zahed, Phys. Rev. Lett. **70**, 3852 (1993), arXiv:hep-th/9303012.
- [36] A. D. Linde, Phys. Lett. B **96**, 289 (1980).
- [37] T. Lappi and L. McLerran, Nucl. Phys. A **772**, 200 (2006), arXiv:hep-ph/0602189.
- [38] F. Gelis, E. Iancu, J. Jalilian-Marian, and R. Venugopalan, Ann. Rev. Nucl. Part. Sci. **60**, 463 (2010), arXiv:1002.0333 [hep-ph].
- [39] J. Berges, K. Boguslavski, S. Schlichting, and R. Venugopalan, Phys. Rev. D **89**, 114007 (2014), arXiv:1311.3005 [hep-ph].
- [40] M. Giordano and T. G. Kovacs, Universe **7**, 194 (2021), arXiv:2104.14388 [hep-lat].
- [41] D. B. Kaplan, Phys. Lett. B **288**, 342 (1992), arXiv:hep-lat/9206013.
- [42] R. V. Gavai, M. E. Jaensch, O. Kaczmarek, F. Karsch, M. Sarkar, R. Shanker, S. Sharma, S. Sharma, and T. Ueding, Phys. Rev. D **111**, 034507 (2025), arXiv:2411.10217 [hep-lat].
- [43] R. Narayanan and H. Neuberger, Nucl. Phys. B **443**, 305 (1995), arXiv:hep-th/9411108.
- [44] H. Neuberger, Phys. Lett. B **417**, 141 (1998), arXiv:hep-lat/9707022.
- [45] T. Kalkreuter and H. Simma, Comput. Phys. Commun. **93**, 33 (1996), arXiv:hep-lat/9507023.
- [46] G. Boyd, J. Engels, F. Karsch, E. Laermann, C. Legeland, M. Lutgemeier, and B. Petersson, Phys. Rev. Lett. **75**, 4169 (1995), arXiv:hep-lat/9506025.
- [47] A. Francis, O. Kaczmarek, M. Laine, T. Neuhaus, and H. Ohno, Phys. Rev. D **91**, 096002 (2015), arXiv:1503.05652 [hep-lat].
- [48] Y. Aoki *et al.* (Flavour Lattice Averaging Group (FLAG)), Eur. Phys. J. C **82**, 869 (2022), arXiv:2111.09849 [hep-lat].
- [49] J. Berges, K. Boguslavski, S. Schlichting, and R. Venugopalan, Phys. Rev. D **89**, 074011 (2014), arXiv:1303.5650 [hep-ph].
- [50] V. Oganessian and D. A. Huse, Phys. Rev. B **75**, 155111 (2007).
- [51] T. G. Kovacs and R. A. Vig, Phys. Rev. D **97**, 014502 (2018), arXiv:1706.03562 [hep-lat].
- [52] N. Chavda and V. Kota, Physics Letters A **377**, 3009 (2013).
- [53] X. Yao, L. Ebner, B. Müller, A. Schäfer, and C. Seidl (2023) arXiv:2312.13408 [hep-lat].
- [54] L. Ebner, A. Schäfer, C. Seidl, B. Müller, and X. Yao, (2024), arXiv:2401.15184 [hep-lat].
- [55] B. Mandelbrot, *The fractal geometry of nature* (Freeman, 1983).
- [56] D. A. Parshin and H. R. Schober, Phys. Rev. Lett. **83**, 4590 (1999).
- [57] K. Jansen and C. B. Lang, Phys. Rev. Lett. **66**, 3008 (1991).
- [58] J. Engels and F. Karsch, Phys. Rev. D **85**, 094506 (2012), arXiv:1105.0584 [hep-lat].
- [59] T. G. Kovacs and F. Pittler, Phys. Rev. Lett. **105**, 192001 (2010), arXiv:1006.1205 [hep-lat].
- [60] T. G. Kovacs and F. Pittler, Phys. Rev. D **86**, 114515 (2012), arXiv:1208.3475 [hep-lat].
- [61] M. Giordano, T. G. Kovacs, and F. Pittler, Phys. Rev. Lett. **112**, 102002 (2014), arXiv:1312.1179 [hep-lat].
- [62] M. Giordano, T. G. Kovacs, and F. Pittler, JHEP **06**, 007 (2016), arXiv:1603.09548 [hep-lat].
- [63] M. Giordano, S. D. Katz, T. G. Kovacs, and F. Pittler, JHEP **02**, 055 (2017), arXiv:1611.03284 [hep-lat].
- [64] L. Holicki, E.-M. Ilgenfritz, and L. von Smekal, PoS **LATTICE2018**, 180 (2018), arXiv:1810.01130 [hep-lat].
- [65] A. Alexandru and I. Horváth, Phys. Lett. B **833**, 137370 (2022), arXiv:2110.04833 [hep-lat].
- [66] M. Giordano, (2022), arXiv:2206.11109 [hep-th].
- [67] R. Kehr, D. Smith, and L. von Smekal, (2023), arXiv:2304.13617 [hep-lat].
- [68] H. T. Ding *et al.* (HotQCD), Phys. Rev. Lett. **123**, 062002 (2019), arXiv:1903.04801 [hep-lat].
- [69] A. Alexandru and I. Horváth, Phys. Rev. D **92**, 045038 (2015), arXiv:1502.07732 [hep-lat].
- [70] A. Alexandru and I. Horváth, Phys. Rev. D **100**, 094507 (2019), arXiv:1906.08047 [hep-lat].
- [71] A. Alexandru and I. Horváth, Phys. Rev. Lett. **127**, 052303 (2021), arXiv:2103.05607 [hep-lat].
- [72] I. Horváth and P. Markoš, Phys. Rev. Lett. **129**, 106601 (2022), arXiv:2110.11266 [cond-mat.dis-nn].
- [73] X.-L. Meng, P. Sun, A. Alexandru, I. Horváth, K.-F. Liu, G. Wang, and Y.-B. Yang (χ QCD, CLQCD), (2023), arXiv:2305.09459 [hep-lat].
- [74] A. Alexandru, I. Horváth, and N. Bhattacharyya, Phys. Rev. D **109**, 014501 (2024), arXiv:2310.03621 [hep-lat].
- [75] L. Y. Glozman, O. Philipsen, and R. D. Pisarski, Eur. Phys. J. A **58**, 247 (2022), arXiv:2204.05083 [hep-ph].
- [76] C. Rohrhofer, Y. Aoki, G. Cossu, H. Fukaya, C. Gattringer, L. Y. Glozman, S. Hashimoto, C. B. Lang, and S. Prelovsek, Phys. Rev. D **100**, 014502 (2019), arXiv:1902.03191 [hep-lat].
- [77] H. Satz, Nucl. Phys. A **642**, 130 (1998), arXiv:hep-ph/9805418.
- [78] P. J. Forrester, Nucl. Phys. B **402**, 709 (1993).
- [79] M. Suzuki, Progress of Theoretical Physics **69**, 65 (1983).
- [80] T. Epelbaum and F. Gelis, Phys. Rev. Lett. **111**, 232301 (2013), arXiv:1307.2214 [hep-ph].
- [81] J. Berges, K. Boguslavski, L. de Bruin, T. Butler, and J. M. Pawłowski, Phys. Rev. D **109**, 114011 (2024), arXiv:2307.13669 [hep-ph].
- [82] A. Kurkela and Y. Zhu, Phys. Rev. Lett. **115**, 182301 (2015), arXiv:1506.06647 [hep-ph].
- [83] B. Muller and A. Trayanov, Phys. Rev. Lett. **68**, 3387 (1992).
- [84] C.-q. Gong, Phys. Lett. B **298**, 257 (1993), arXiv:hep-lat/9209018.
- [85] T. S. Biro, C. Gong, and B. Muller, Phys. Rev. D **52**, 1260 (1995), arXiv:hep-ph/9409392.
- [86] J. Berges, M. Mace, and S. Schlichting, Phys. Rev. Lett. **118**, 192005 (2017), arXiv:1703.00697 [hep-th].
- [87] P. A. Baikov, K. G. Chetyrkin, and J. H. Kühn, Phys. Rev. Lett. **118**, 082002 (2017), arXiv:1606.08659 [hep-ph].
- [88] T. Kunihiro, B. Muller, A. Ohnishi, A. Schafer, T. T. Takahashi, and A. Yamamoto, Phys. Rev. D **82**, 114015 (2010), arXiv:1008.1156 [hep-ph].
- [89] D. Bala, O. Kaczmarek, P. Petreczky, S. Sharma, and S. Tah, Phys. Rev. Lett. **135**, 012301 (2025), arXiv:2501.17943 [hep-lat].
- [90] U. W. Heinz, AIP Conf. Proc. **739**, 163 (2004), arXiv:nucl-th/0407067.

- [91] S. Sharma, PoS **CPOD2017**, 086 (2018).
- [92] M. P. Lombardo and A. Trunin, Int. J. Mod. Phys. A **35**, 2030010 (2020), arXiv:2005.06547 [hep-lat].
- [93] M. A. Clark, R. Babich, K. Barros, R. C. Brower, and C. Rebbi (QUDA), Comput. Phys. Commun. **181**, 1517 (2010), arXiv:0911.3191 [hep-lat].